J. Bandyopadhyay[1], S. A. Al-Thabaiti[2], S. S. Ray[1,2,3], M. Bousmina[4]*

[1] *DST/CSIR National Centre for Nanostructured Materials, Council for Scientific and Industrial Research, Pretoria, South Africa*
[2] *Department of Chemistry, King Abdulaziz University, Jeddah, Kingdom of Saudi Arab*
[3] *Department of Applied Chemistry, University of Johannesburg, Johannesburg, South Africa*
[4] *Euro-Mediterranean University of Fez and Hassan II Academy of Science and Technology, Rabat, Morocco*

Viscoelastic and Electrical Properties of Carbon Nanotubes Filled Poly(butylene succinate)

The carbon nanotubes (CNTs)-containing composites of poly(butylene succinate) (PBS) were prepared by melt-blending in a batch mixer with three concentrations by weight of CNTs: 1, 2 and 3 %. State of dispersion-distribution of the CNTs in the PBS matrix was examined by electron microscopic observations that revealed homogeneous distribution of agglomerated CNTs in PBS matrix. The dynamic mechanical studies demonstrated an increase in the storage modulus of PBS matrix with the CNTs loading. Melt-state rheological properties measurements were found to be modified with CNT loading changing from liquid-like, to gel-like and then to viscoelastic solid-like. Finally, the in-plane electrical conductivity was found to be substantially enhanced with CNT loading, whereas the through-plane conductivity was found to be only slighted increased with the CNT loading. Such changes in viscoelastic properties along with the improvements in both thermomechanical and electrical properties are expected to open opportunities for the use of PBS extending its applications from the classical field of packaging to new niches such as tissue-engineering.

1 Introduction

Poly(butylene succinate) (PBS) is a biodegradable linear aliphatic polyester, generally synthesized by the polycondensation of 1, 4-butanediol with succinic acid. PBS has excellent processability, so it can be processed in the field of textiles into melt blow, multifilament, monofilament, nonwoven, flat, and split yarn and also in the field of plastics into injection-molded products, thus being a promising polymer for various potential applications (Ishioka et al., 2002). However, other properties of PBS, such as melt viscosity for further processing is often not sufficient to extend its application to other niches.

Because of their inherent extraordinary high strength and high modulus, their excellent electrical conductivity along with their important thermal conductivity and stability and their low density (Dresselhaus, 1996), carbon nanotubes (CNTs) have been extensively used for the preparation of conducting polymer composites with balanced mechanical properties.

Recently, a number of articles have appeared on the preparation, characterization, and evaluation of properties of CNTs- or clay-reinforced PBS composites (Ray et al., 2003; 2006a; 2007a; 2007b; 2007c; Ray and Bousmina, 2005; 2006b; 2006c). For instance, Ray et al. (2006a) first reported the preparation, characterization and properties of multi-walled CNTs (MWCNTs) containing PBS composites. The tensile modulus of PBS was significantly improved after incorporation of 3 wt.% of MWCNTs, however, a dramatic loss of toughness and strength of composite was noted. Shih et al. (2008) studied the effect of MWCNTs surface functionalization on the crystallization behavior and thermo-mechanical properties of PBS. The MWCNTs surface was modified with N,N′-dicyclohexylcarbodiimide (DCC) dehydrating agents. The obtained results showed some degree of improvement in the dynamic mechanical properties of PBS after incorporation of functionalized MWCNTs. In another report, Ali and Mohan (2009) studied the effect of incorporation MWCNTs on thermal, mechanical, and rheological properties of PBS matrix. The results showed that elongation-at-break decreased and modulus increased with increasing the amount of MWCNTs in the PBS/MWCNTs composites. Song and Qiu (2010) and Shih (2009) studied the effect of incorporation of MWCNTs on the non-isothermal crystallization behavior of PBS matrix and found that MWCNTs act as a nucleating agent for the crystallisation PBS matrix.

In summary, most of the reported works have focused on enhanced storage and tensile moduli, thermal and electrical properties, and non-isothermal crystallization behavior of the final composite materials. However and to the best of our knowledge, detailed melt-state rheological properties have not been studied in the case of PBS/CNTs nanocomposites.

Therefore, the main objective of this work is to report on the viscoelastic and electrical properties of MWCNTs-containing nanocomposites of PBS. The obtained results are discussed in terms of the state of dispersion and distribution of the CNTs within the PBS matrix.

* Mail address: Suprakas Sinha Ray, DST/CSIR National Centre for Nanostructured Materials, Council for Scientific and Industrial Research, Pretoria 0001, South Africa
E-mail: rsuprakas@csir.co.za

2 Experimental

2.1 Materials

PBS used in this study is a commercial product from Showa High Polymer (Japan), with the designation Bionolle #1020, which has, according to the supplier, a weight average molecular weight, M_w = 103 kg/mol, melt flow index (MFI) = 2.5 gm/10 min (190 °C, 2.16 kg), and melting temperature, T_m = 115 °C. To increase the interfacial interactions with the surface of treated CNTs, PBS was modified by a coupling reaction of relatively low molecular weight PBS in the presence of hexamethylenediisocyanate ($OCN-C_6H_{12}-NCO$) as a chain extender. A typical formulation consisted of 4.07 kg of hexamethylenediisocyanate that was added to the reactor containing 339 kg of PBS (number average molecular weight, M_n and weight average molecular weight, M_w are 18.6 and 50.3 kg/mol, respectively) to perform a coupling reaction for 1 h at 180 to 200 °C. Each PBS chain has 0.48 wt.% of chain extender and this group makes urethane type bonds (refer to Fig. 1) with hydroxy-terminated PBS having low molecular weight. The obtained final M_n and M_w were 42 and 101 kg/mol, respectively.

The MWCNTs used in this study were synthesized by chemical vapor deposition (CVD) method in our laboratory. To introduce some active groups such as carboxylic acid (COOH) on the surface of the CNTs, the as synthesized MWCNTs (p-MWCNTs) were first refluxed in 5 M HNO_3 for 1 h. Subsequently, oxidized MWCNTs (o-MWCNTs) were washed with distilled water and acetone and dried under vacuum at 100 °C before their melt-blending with PBS matrix.

The formation of carboxylic acid groups on the outer graphene layer of the MWCNTs could be identified by comparing the X-ray photoelectron spectroscopy (XPS) spectra of p-MWCNTs and o-MWCNTs. Figure 2 presents the XPS spectra of p-MWCNTs and o-MWCNTs samples. Two features can be identified from XPS spectra; first is the appearance of strong "O 1s" and "O KLL" peaks in the XPS spectrum of o-MWCNTs, which are attributed to the presence of "COOH" groups on the MWCNTs outer surfaces. Second, the characteristic "C 1s" peak of p-MWCNTs shifts towards the lower binding energy side in the case of o-MWCNTs (refer to Fig. 2B), indicating that the o-MWCNTs' surface carbon atoms are less stabilized than those of p-MWCNTs as a result of oxidation.

2.2 PBS/CNT Composite Processing

PBS/o-MWCNTs (from now on o-MWCNTs are abbreviated as CNTs) composites containing three different wt.% CNTs were prepared via melt-blending using a co-rotating twin rotor thermohaake batch-mixer (Polylab system) operated at 150 °C (set temperature) and a rotor speed of 60 min^{-1} for 8 min. CNTs were slowly added after two and half min of melting of PBS inside the mixer, which was considered as time zero. The dried composite strands were then converted into sheets with a thickness of 0.4 to 1.5 mm by compression molding at 2 torr pressure and 160 °C for 2 min using the Craver Laboratory Press. For dynamic mechanical property measurements, neat PBS and PBS/CNT composite samples (compression molded) were annealed overnight at 50 °C under vacuum. The PBS/CNTs composites containing 1, 2, and 3 wt.% of CNTs are abbreviated here by PBS1CNT, PBS2CNT and PBS3CNT.

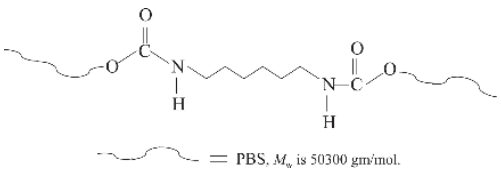

Fig. 1. Formation of urethane bonds in high molecular weight PBS

2.3 Surface Morphology and Dispersion Characteristic

Scanning electron microscopy analyses were conducted on freeze-fractured surfaces of the compression molded composites. Prior to observations, the fractured surfaces were sputter-coated with gold/palladium alloy to minimise charging, and their surface morphology was studied using a scanning electron microscope (SEM, Carl Zeiss, Germany) at an accelerating voltage of 3 kV.

Dispersion and distribution of the CNTs in the PBS matrix were evaluated by means of transmission electron microscopy (TEM, JEOL model JEM-1230 instrument) operated at an accelerating voltage of 80 kV. The TEM specimens were about 100 nm thick and were prepared by ultramicrotoming the composite samples encapsulated in epoxy matrix with a diamond knife.

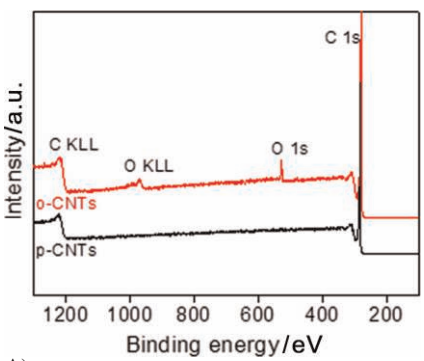

A)

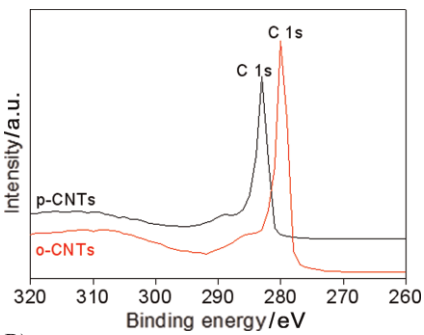

B)

Fig. 2. (A) X-ray photoelectron spectroscopic scans of p-MWCNTs and o-MWCNTs samples, (B) zoomed version of peak C1s

2.4 Dynamic Property Measurement

Dynamic mechanical properties of neat PBS and composites with three different CNT loadings were measured by using a Rheometrics Scientific Analyzer (RSA) in the dual cantilever bending mode. The temperature dependence of storage flexural modulus (E′) of neat PBS and composites was measured at a constant frequency (ω) of 6.28 rad/s with a strain amplitude of 0.02 % (within liner range, selected after a series of tests at three different temperatures) and in the temperature range of –50 to 100 °C with a heating rate of 2 °C/min.

2.5 Melt Rheology

Melt rheological measurements were performed on Paar-Physica MCR 500 Rheometer in parallel plate geometry using 25 mm diameter parallel plates. All tests were conducted at 160 °C. Linear viscoelastic zone was assessed by performing strain sweep tests both at small and high frequencies. Frequency sweep tests from 0.01 to 100 rad/s were performed at 0.2 % strain under nitrogen atmosphere.

2.6 Electrical Property

Electrical properties were measured by use of a Keithley 220-programable current source and 181-nanovoltameter, which was controlled by a computer. Samples used in conductivity measurements were in the form of a rectangular sheet of around 0.1 mm thickness obtained by compression molding.

3 Results and Discussions

3.1 Analyses of the State of Dispersion and Distribution of CNTs

The state of dispersion-distribution of CNTs within PBS matrix was analysed by both SEM and TEM techniques. Several zones of the composites were observed by electron microscopy and the provided micrographs were selected to faithfully represent the overall state of dispersion distribution. Typical SEM and TEM micrographs of the composites for the three CNT concentrations are shown in Figs. 3 and 4.

SEM observations reveal that the CNTs have a characteristic length of several microns and due to their high aspect ratio and their bending capacity, they form local interconnections and entanglement-like structure favored by important surface van-der Waals interactions. This leads to some local clusters with a size that increases with the CNT concentration. Two features are noted: (i) dispersion and (ii) distribution. Dispersion concerns the possibility of reducing the size of the clusters and distribution concerns the spatial homogeneous partition such clusters. TEM observations show that for all concentrations, CNT nanoparticles are well distributed within the PBS matrix, while the dispersion is slightly reduced upon increase in concentration, with the appearance of larger clusters for PBS3CNT. This was an expected result since the percolation threshold of these high aspect-ratio CNT is very small and any concentration exceeding such a threshold would lead to the formation of local clusters. TEM micrographs show also some orientation of the clusters (which is more evident for PBS3CNT) due to the compression molding.

3.2 Dynamic Mechanical Properties

Dynamic mechanical analyses provide the thermomechanical material response under a periodic stress with variation of time, temperature or frequency of oscillations. The current study focuses on the variation of the E′ as a function of temperature. The results in terms of E′ and tanδ are presented in Fig. 5. At low temperature, PBS matrix and the corresponding composites do show a high modulus of order of GPa. PBS has a low-

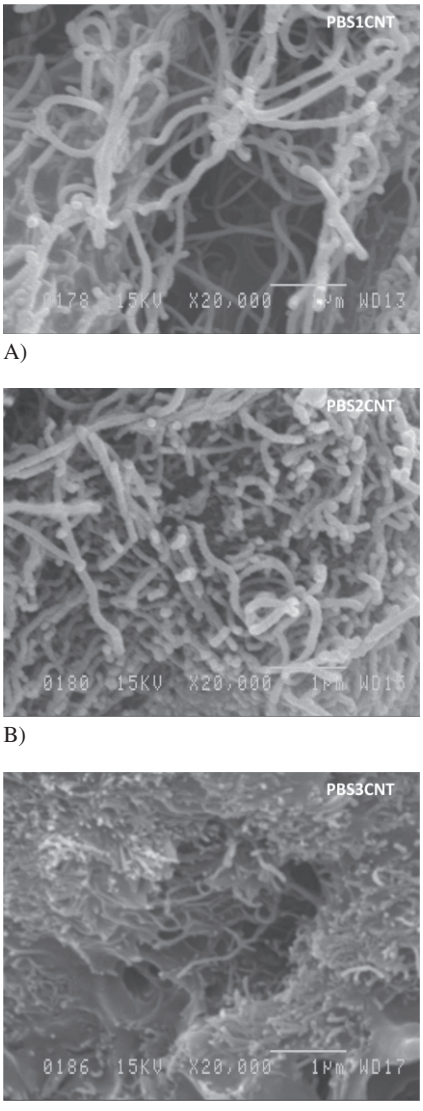

Fig. 3. Scanning electron microscopy images of freeze-fractured surface of (A) PBS1CNT, (B) PBS2CNT and (C) PBS3CNT. The scale bars indicate 1 μm

temperature modulus of about 3.5 GPa. Such a modulus increases to about 5 GPa for PBS1CNT and PBS2CNT and then decreases to about 4.2 GPa for PBS3CNT. Such a result is in accordance with the formation of larger clusters revealed by TEM analyses. The clustering is favored both by steric interactions and by van-der Waals surface forces leading to micronic domains that confer to the two-phase system a composite-like structure rather than nanocomposite one. This induces a high concentration of the local stresses at the interface between the homogeneous matrix and the micronic domains, which is responsible for low temperature fragile behavior.

The increase in temperature facilitates the molecular motion and switches the behavior from glassy to rubbery and then to viscous at very high temperature. Such viscous behavior is only apparent and an extension of the temperature range would show a plateau at high temperature due to the formation of three-dimensional percolated network. This point will be discussed later.

The rubbery plateau for both PBS matrix and PBS/CNTs is not clearly defined, denoting low density of entanglements due to side chains obtained through the chemical modification of PBS. However, the plateau region is more prominent in the composites than in the PBS matrix due to the contribution of the clusters and interconnections of the CNT nanoparticles.

Although the glass transition occurs in a wide interval of temperature, the glass transition temperature can be determined from the tanδ (ratio of loss modulus to the storage modulus) peak position. According to Fig. 5B, the glass transition temperature of neat PBS remains unaltered after composite formation. Therefore, the relative increase in E′ is not due to any modification in glass transition temperature, but it is rather related to the dispersion-distribution of CNTs within the PBS matrix. However, CNTs have an extremely high strength (about 60 GPa) and high modulus (0.3 to 1 TPa) and the relative enhancement obtained through their addition within PBS is not significant, although their good distribution within the PBS matrix. In fact to get high benefit from the high modulus of CNTs, distribution is not enough; dispersion, orientation and strong matrix-CNT interfacial adhesion are of crucial importance.

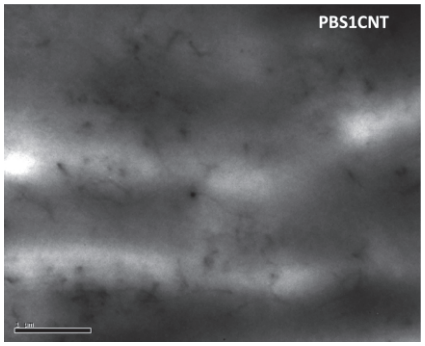

A)

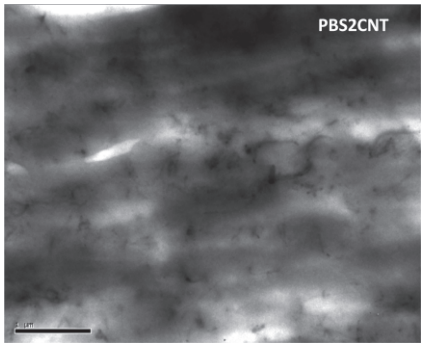

B)

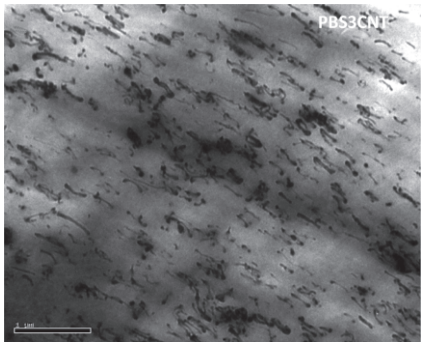

C)

Fig. 4. Transmission electron microscopic images of (A) PBS1CNT, (B) PBS2CNT and (C) PBS3CNT. The scale bars indicate 1 μm

3.3 Melt-State Rheology

Oscillatory shear flow experiments were conducted in three configurations: i) strain sweep, ii) frequency sweep and iii)

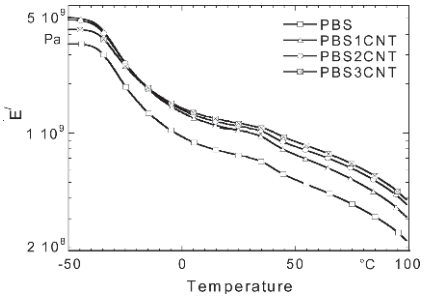

A)

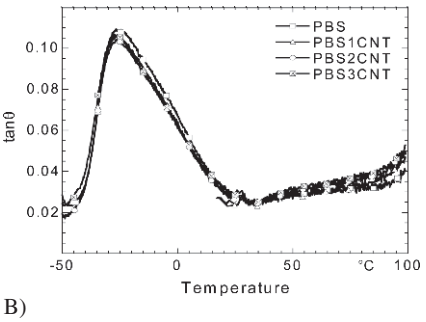

B)

Fig. 5. Variation of the dynamic flexural modulus (A) and tanδ (B) as a function of temperature in the range –50 to 100 °C for neat PBS and three different CNTs-containing PBS composites. Experiments were conducted at a constant frequency, ω, of 6.28 rad/s with a strain amplitude of 0.02 % (selected after a series of strain sweep tests at different temperatures to determine the linear region) and in the temperature range of –50 to 100 °C at a heating rate of 2 °C min^{-1}

temperature sweep. Then relation experiments were conducted as a function of time at 160 °C and a strain of 0.2 %.

3.3.1 Amplitude Sweep

Strain sweep experiments were performed at 160 °C in nitrogen atmosphere with a constant angular frequency of 6.28 rad/s and in the strain region of 0.005 to 100 %. As demonstrated in Fig. 6, the response of all samples does not depend on the strain (both the storage modulus, G′ and loss modulus, G″, exhibit a constant plateau), and the behavior is well within the linear viscoelastic (LVE) region. However, the plateau region shortens with the CNTs loading in the composites when compared with neat PBS.

It's also noteworthy to notice that in case of neat PBS, G″ is dominating over G′, indicating that the overall behavior of the matrix is dominated by viscous segmental frictions. PBS1CNT exhibits quite similar trend as neat PBS, with however less difference between the magnitudes of G″ and G′. In PBS2CNT G″ and G′ are almost overlapping and in PBS3CNT G′ becomes higher than G″, denoting a gradual switch from viscoelastic liquid-like to solid-like behavior.

In fact, neat PBS shows liquid-like character in the whole strain range and the incorporation of CNTs modifies the chains relaxation and hinders the chains flow. This induces two modifications: First the LVE region is shortened with the increase in CNT loading bringing the LVE limit from 10 % for PBS1CNT to 3 % and then to 1 % for PBS2CNT and PBS3CNT, respectively. The second modification concerns the gap between G″ and G′, which is large for PBS and PBS1CNT (liquid-like behavior: G″ > G′), becoming quite zero for PBS2CNT (Gel-like behavior: G″ ∼ G′) and reverting for PBS3CNT (viscoelastic solid-like behavior: G′ > G″). From the above experiments, the strain was then set at 0.2 % to ensure that the response of all materials is within the LVE region.

3.3.2 Small Amplitude Oscillatory Shear Flow (Frequency Sweep)

Small amplitude oscillatory shear measurements were conducted at a temperature of 160 °C and a strain of 0.2 %. The obtained dynamic moduli, G′ and G″, are presented in Fig. 7 for PBS and for the corresponding composites. The obtained behavior in frequency sweep is in accordance with the results of strain sweep. In fact, PBS and PBS1CNT exhibit G″ > G′ throughout the examined frequency range. This indicates a viscous behavior for both cases, with however a clear difference in the variation of the dynamic moduli with the frequency. In fact, PBS shows a Maxwellian terminal-zone like behavior, with G′ and G″ decreasing linearly with lowering of frequency in log-log scale, with a slope of 2 and 1, respectively, whereas the slopes in the case of PBS1CNT are quite similar, a behavior that is characteristic of gel-like materials. For PBS3CNT, G′ becomes larger than G″ and both reach a low-frequency plateau characteristic of solid-like behavior due to a three-dimensional percolating network of CNT clusters (Bousmina and Muller 1996; Grmeal et al., 2001; Eslami et al., 2007). TEM micrographs did show a 2-D microstructure formed by the spatial distribution of clusters with different sizes and with a small inter-cluster average distance. Actually, a 3-D view would show a percolating network leading to the observed solid-like behavior as was somewhat revealed by SEM analyses.

The variation of the complex shear viscosity as a function of frequency is another way to represent the results. While, PBS shows a constant viscosity in the low-frequency region, the composites show a frequency-thinning behavior (similar to shear-thinning behavior), with an increase in viscosity in the low-frequency region. The presence of CNT clusters network inhibits disentanglement and polymer chains flow.

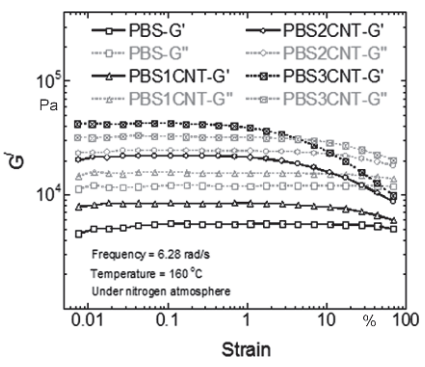

Fig. 6. Strain sweep results of neat PBS and its composites containing three different wt.% of CNTs. The experiments were performed at 160 °C in nitrogen atmosphere with a constant angular frequency of 6.28 rad/s

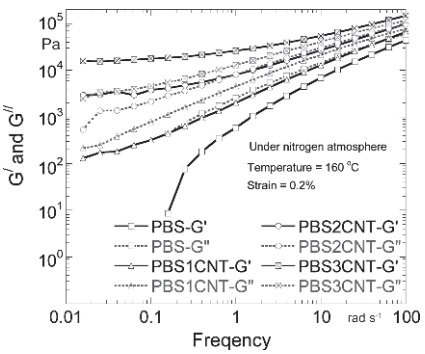

A)

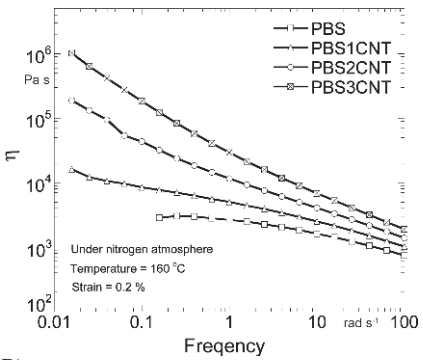

B)

Fig. 7. Variation of the dynamic moduli G′ and G″ (A) and the complex shear viscosity (B) as a function of frequency for neat PBS and its composites. The experiments were performed at 160 °C in a nitrogen atmosphere with a constant strain of 0.2 %

3.3.3 Temperature Sweep

To enlarge the temperature range of the thermo-mechanical behavior of both PBS and the composites, G′ was measured as a function of temperature at a frequency of 6.28 rads/s and a strain of 0.2 %. Such experiments extend somewhat the results shown in Fig. 5 to higher temperature, since shear and flexural moduli are related. The results are reported in Fig. 8. It is clearly seen that the shear modulus of both PBS and PBS1CNT decrease with temperature (viscous flow behavior), with a rate that is higher for PBS. In contrast, PBS2CNT and PBS3CNT show only a marginal decrease as a function of temperature, with G′ being almost constant. The G′-values corresponding to the temperature 160 °C are similar to those obtained in Figs. 6 and 7 at the same frequency of 6.28 rads/s. For instance G′ of PBS2CNT and PBS3CNT are approximately equal to 2.10^4 Pa and 5.10^4 Pa, respectively for the three experiments at the same temperature of 160 °C and same frequency of 6.28 rads/s. Since in each experiment, a new fresh sample was loaded in the rheometer, this proves that the used mixing conditions led to reproducible steady state macroscopic dispersion and distribution of CNTs within the PBS matrix (as was also verified by constant torque during batch-mixing). The observed pseudo-plateau on G′ for PBS2CNT and PBS3CNT extends over the entire tested temperature range, with only a marginal decrease from 150 to 190 °C. Within this temperature range, the energy of activation is very small and the build-up of the percolating network is quite insensitive to thermal activation. Normally and similarly to rubbery elastic behavior (rubber elasticity theory), from such a pseudo-plateau, it is possible to extract the density of contacts or the number of clusters between two contacts in the percolating network of the dispersed CNTs.

3.3.4 Stress Relaxation

Stress relaxation experiments that are quite often more sensitive than steady state ones in multiphase systems (Iza and Bousmina 2000) were conducted at a constant strain of 0.2 % and at a temperature 160 °C. The variation of the relaxation modulus in time is reported in Fig. 9. The results show that G(t) of PBS drops rapidly and vanishes for long time at around 100 s (viscoelastic liquid behavior), whereas for composites, G(t) extends to long time and reaches a finite pseudo-plateau with a magnitude that increases with the concentration of CNT. This is another indication for the formation of a 3-D percolating network leading to a viscoelastic-solid behavior. The stress in such percolating network is not completely relaxed and the residual stress ($\sigma_r = \sigma_0 - \sigma_e = (G_0 - G_e)/\gamma_0$) translates both the density of the network formed by the solid CNT-clusters and the concentration of the PBS polymer chains entrapped within the network that participate to the incomplete relaxation process.

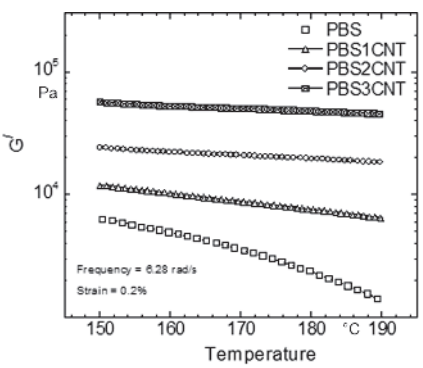

Fig. 8. Variation of the dynamic storage modulus, G′, a function of temperature for PBS and various CNTs-containing PBS nancomposites. The experiments were performed with a constant angular frequency 6.28 rad/s in nitrogen atmosphere

3.4 Electrical Conductivity

The electrical conductivity of neat PBS and PBSCNTs are reported in Table 1. For all samples, the in-plane electrical conductivity was found to be substantially enhanced with CNT loading, whereas the through-plane conductivity was found to be only slighted increased with the CNT loading. This is an indication of important orientation of CNT nanoparticles due to the molding of the samples. Although, the composites are characterized by a 3-D percolating network, such a network is distorted with a new orientation in the plane of the sample. The

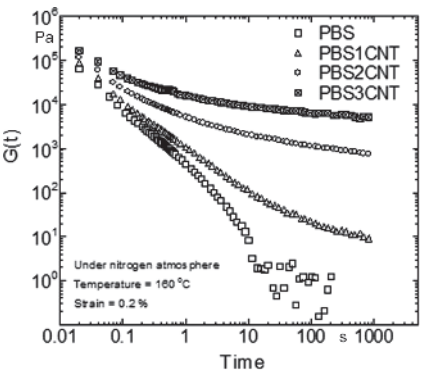

Fig. 9. Variation of the relaxation modulus in time for neat PBS and PBS/CNTs nanconposites. The experiments were performed with a constant strain of 0.2 % in nitrogen atmosphere

Sample	Conductivity/S cm^{-1}	
	in plane	through plane
PBS	5.6×10^{-9}	4.5×10^{-11}
PBS1CNT	8.4×10^{-5}	1.2×10^{-9}
PBS2CNT	7.3×10^{-4}	7.1×10^{-9}
PBS3CNT	4.4×10^{-3}	9.9×10^{-8}

Data presented here are average values of three independent measurements

Table 1. Electrical conductivity of neat PBS and its CNTs-containing composites

addition of CNT induces a spectacular increase in the in-plane conductivity of the PBS matrix (about 10^6 times increase).

4 Concluding Remarks

The state of dispersion-distribution of CNT nanoparticles within PBS matrix was characterized by SEM and TEM microscopy and thermo-rheological and electrical analyses. The electron microscopy results showed that the melt-mixing process led to a medium quality of dispersion of CNT nanoparticles within the PBS matrix that form mostly sub-micronic clusters. However, TEM analyses combined with rheological characterisation have revealed homogeneous spatial distribution of CNT aggregates within the PBS matrix. Such state of dispersion-distribution resulted in important modifications in thermo-rheological behavior of the composites, changing gradually from liquid-like, to gel-like and then to solid-like like behavior for high CNT loading (3 wt.%). Such solid-like behavior is inferred to a 3-D percolated network of CNT nanoparticles, with however, some distortion and privileged in-plane orientation (due to the preparation of the samples by compression molding) that results in a spectacular increase of in-plane electrical conductivity.

References

Ali, F. B., Mohan, R., "Thermal, Mechanical, and Rheological Properties of Biodegradable Polybutylene Succinate/Carbon Nanotubes Nanocomposites", Polym. Compos., **31**, 1309–1314 (2010)

Bousmina, M., Muller, R., "Rheology/Morphology/Flow Conditions Relationships for Polymethylmethacrylate/Rubber Blend", Rheol. Acta, **35**, 369–381 (1996), DOI:10.1007/BF00403538

Dresselhaus, M. S., Dresselhaus, G. and Eklund, P. C.: Science of Fullerenes and Carbon Nanotubes, Academic Press, San Diego (1996)

Eslami, H., Grmela, M. and Bousmina, M., "Mesoscopic Rheological Model of Layered Silicate Nanocomposites", J. Rheol. **51**, 1189–1222 (2007), DOI:10.1122/1.2790461

Grmela, M., Bousmina, M. and Palierne, J. F., "On The Rheology of Immiscible Blends". Rheol. Acta, **40**, 560–569 (2001), DOI:10.1007/s003970100188

Hoffmann, B., Kressler, J., Stöpplmann, G., Friedrich, Chr. and Kim, G. M., "Rheology of Nanocomposites Based on Layered Silicate and Polyamide-12", Colloid Polym. Sci., **278**, 629–636 (2000), DOI:10.1007/s003960000294

Ishioka, D. R., Kitakuni, E. and Ichikawa, Y., "Volume 4 Aliphatic Polyesters: Bionolle, Biopolymers, in Polyesters III. Application and Commercial Products, Doi, Y., Steinbuchel, A. (Eds.), Wiley-VCH, Weinheim, p. 275–297 (2002)

Iza, M., Bousmina, M., "Nonlinear Rheology of Immiscible Polymer Blends: Step Strain Experiments", J. Rheol., **44**, 1363–1384 (2000), DOI:10.1122/1.1308521

Iza, M., Bousmina, M., Jerome, R. "Rheology Of Compatibilized Immiscible Viscoelastic Polymer Blends", Rheologica Acta. **40**, 10–22 (2001), DOI:10.1007/s003970000112

Song, L., Qiu, Z., "Biodegradable Poly(butylene succinate)/Multi-Walled Carbon Nanotubes Nanocomposite at Low Carbon Nanotubes Loading: Morphology, Crystallization and Mechanical Property", J. Nanosci. Nanotechnol.,**10**, 965–972 (2010), PMid:20352743; DOI:10.1166/jnn.2010.1815

Shih, Y. F., Chen, L. S. and Jeng, R. J., "Preparation and Properties of Biodegradable PBS/Multi-Walled Carbon Nanotubes Nanocomposites", Polymer **49**, 4602–4611 (2008), DOI:10.1016/j.polymer.2008.08.015

Shih, Y. F., "Thermal Degradation and Kinetic Analysis of Biodegradable PBS/Multiwalled Carbon Nanotube Nanocomposites", J. Polym. Sci. Part B: Polym. Phys. **47**, 1231–1239 (2009), DOI:10.1002/polb.21728

Ray, S. S., Okamoto, K. and Okamoto, M., "Structure-Property Relationship in Biodegradable Poly(butylene succinate)/Layered Silicate Nanocomposites", Macromolecules, **36**, 2355–2367 (2003), DOI:10.1021/ma021728y

Ray, S. S., Bousmina, M., "Biodegradable Polymers and their Layered Silicate Nanocomposites: In Greening the 21st Century Materials World", Prog. Mater. Sci., **50**, 962–1079 (2005), DOI:10.1016/j.pmatsci.2005.05.002

Ray, S. S., Vaudreuil, S., Maazouz, A. and Bousmina, M., "Dispersion of Multi-Walled Carbon Nanotubes in Biodegradable Poly(butylene succinate) Matrix", J. Nanosci. Nanotechnol., **6**, 2191–2195 (2006a), PMid:17025148; DOI:10.1166/jnn.2006.368

Ray, S. S., Bousmina, M., "Crystallization Behavior of Poly (butylene succinate)Co-Adipate Nanocomposite", Macromol. Chem. Physics, **207**, 1207–1219 (2006b), DOI:10.1002/macp.200600163

Ray, S. S., Bousmina, M., "The Relations Between Structure and Mechanical Properties of Poly(butylene succinate-co-adipate)/Montmorillonite Nanocomposites", J. Polym. Eng., **26**, 885–901 (2006c)

Ray, S. S., Bousmina, M. and Bandyopadhyay, J., "Effect of Organoclay on the Morphology and Properties of Poly(propylene)/Poly[(butylene succinate)-co-adipate] Blends", Macromol. Mater. Eng., **292**, 729–747 (2007a), DOI:10.1002/mame.200700029

Ray, S. S., Bousmina, M. and Bandyopadhyay, J., "Thermal and Thermomechanical Properties of Poly (butylene succinate)-co-adipate Nanocomposite", Polym. Degr. Stab., **92**, 802–812 (2007b), DOI:10.1016/j.polymdegradstab.2007.02.002

Ray, S. S., Bousmina, M. and Bandyopadhyay, J., "Influence of Degree of Intercalation on the Crystal Growth Kinetics of Poly(butylene succinate)-co-adipate Nanocomposites", Eur. Polym. J., **44**, 3133–3145 (2008), DOI:10.1016/j.eurpolymj.2008.07.035

Acknowledgements

The authors would like thank CSIR, DST and NRF for financial support and the Hassan II Academy of Science and Technology.

Date received: May 02, 2013
Date accepted: November 08, 2013

Bibliography
DOI 10.3139/217.2812
Intern. Polymer Processing
XXIX (2014) 1; page 88–94

ISSN 0930-777X